

DBD Dyes as Fluorescence Lifetime Probes to Study Conformational Changes in Proteins

Robert Wawrzinek,^[a] Joanna Ziomkowska,^[b] Johanna Heuveling,^[b] Monique Mertens,^[a] Andreas Herrmann,^{*[b]} Erwin Schneider,^{*[b]} and Pablo Wessig^{*[a]}

Abstract: Previously, [1,3]dioxolo[4,5-*f*]-[1,3]benzodioxole (DBD)-based fluorophores used as highly sensitive fluorescence lifetime probes reporting on their microenvironmental polarity have been described. Now, a new generation of DBD dyes has been developed. Although they are still sensitive to polarity, in contrast to the former DBD dyes, they have extraordinary spectroscopic properties even in aqueous surroundings. They are characterized by long fluorescence lifetimes (10–20 ns), large Stokes shifts (≈ 100 nm), high photostabilities, and high quantum yields (> 0.56). Here, the spectroscopic prop-

erties and synthesis of functionalized derivatives for labeling biological targets are described. Furthermore, thio-reactive maleimido derivatives of both DBD generations show strong intramolecular fluorescence quenching. This mechanism has been investigated and is found to undergo a photoelectron transfer (PET) process. After reaction with a thiol group, this fluorescence

quenching is prevented, indicating successful bonding. Being sensitive to their environmental polarity, these compounds have been used as powerful fluorescence lifetime probes for the investigation of conformational changes in the maltose ATP-binding cassette transporter through fluorescence lifetime spectroscopy. The differing tendencies of the fluorescence lifetime change for both DBD dye generations promote their combination as a powerful toolkit for studying microenvironments in proteins.

Keywords: dyes/pigments • electron transfer • fluorescent probes • maleimides • MalF • photoelectron transfer

Introduction

Although there are many different commercially available fluorescent dyes, the demand for new fluorophores is still high. There is no universal dye that possesses all the desirable characteristics (high quantum yield, long fluorescence lifetime, high molar extinction coefficients, photostability, low toxicity, etc.), so it is important to enrich the toolbox of luminescent probes so that as many combinations as possible of those parameters are available, preferably for various absorption and emission wavelengths. Fluorescence spectroscopy is developing continuously, and more and more sensitive techniques require specialized probes to realize the ever-higher resolution of small structures and fast processes.

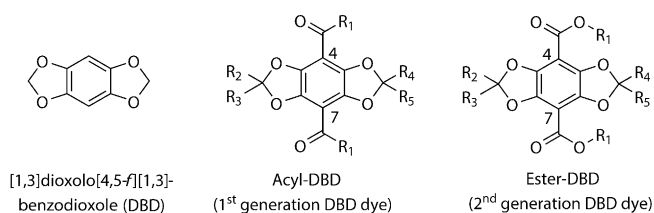
Time-correlated single-photon counting (TCSPC) spectroscopy and fluorescence-lifetime imaging microscopy (FLIM) detect the fluorescence decay of fluorophores at their emission maxima, giving high-contrast signals that are unaffected by decreasing dye concentrations caused by photobleaching.^[1–4] Therefore, the quantitative analysis of fluorescence lifetime spectroscopy is superior to and more accurate than most steady-state techniques, which use fluorescence intensity as a measurement parameter.

The most established fluorophores are based on pyrene, xanthene, coumarin, or oxazine, and are used successfully in countless applications and experiments.^[5–8] However, owing to a lack of availability or even knowledge of more suitable dyes, the resulting data are often not as convincing as desired. In this article, we give an example of why it is still worth investigating new types of fluorophores. In previous work, we introduced new fluorescent dyes based on [1,3]dioxolo[4,5-*f*][1,3]benzodioxole (DBD).^[9,10] We have shown that they could be used as sensitive fluorescence lifetime probes in cell-staining experiments reporting on the polarity of their microenvironment.^[11] Herein, we describe a new generation of DBD dyes containing different electron-withdrawing groups (EWGs) at the 4- and 7-positions of the fluorophore. Scheme 1 shows the general structures of the fluorophores described in this article. They are provided with various functional groups that can be linked to biomolecules. Furthermore, maleimido derivatives of both DBD dye generations were used as powerful probes to in-

[a] R. Wawrzinek, M. Mertens, Prof. Dr. P. Wessig
Institut für Chemie, Universität, Potsdam Karl-Liebknecht-Str. 24-25
14476 Potsdam (Germany)
Fax: (+49) 331-977-5065
E-mail: Wessig@uni-potsdam.de

[b] J. Ziomkowska, Dr. J. Heuveling, Prof. Dr. A. Herrmann,
Prof. Dr. E. Schneider
Institut für Biologie, Humboldt-Universität zu Berlin
Invalidenstraße 42, 10115 Berlin (Germany)
E-mail: h1211dyz@rz.hu-berlin.de
erwin.schneider@rz.hu-berlin.de

Supporting information for this article is available on the WWW under <http://dx.doi.org/10.1002/chem.201302368>.



Scheme 1. General structure of DBD dyes.

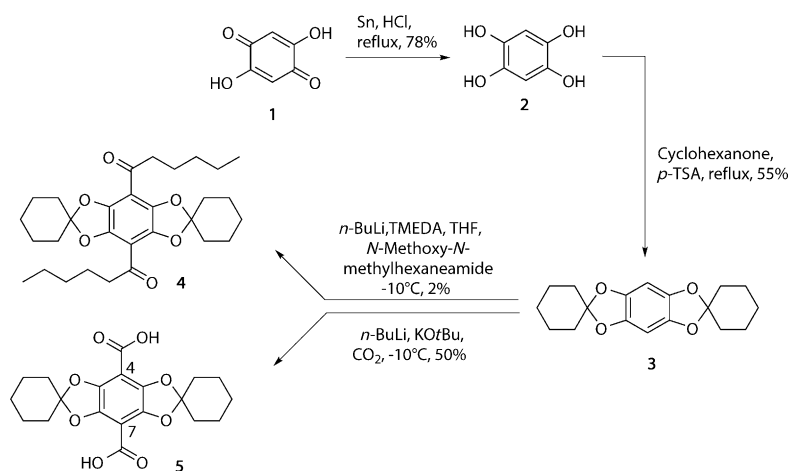
investigate the conformational change of the maltose ATP-binding cassette (ABC) transporter.^[12] In addition, we examined the quenching mechanism of DBD dyes caused by a conjugated maleimide.

Because the previously described acyl-DBD dyes already possess a large number of desired parameters, such as small molecule size, non-toxicity, high photostability, large Stokes shifts, and long fluorescence lifetimes (at least in non-polar microenvironments), we aimed to add new items to the toolbox by developing additional DBD dyes with other interesting characteristics.

Results and Discussion

Synthesis and spectroscopy of new DBD dyes: Although DBD dyes with acyl residues as EWGs are sensitive polarity probes, we considered that different EWGs might reduce the observed strong fluorescence intensity and lifetime quenching in the presence of water to extend their application field. The latter effect is probably caused by hydrogen bridge bonds disturbing the push-pull system of the acyl-DBD dye. Our first substitution of these acyl residues was with carboxylic groups at positions 4 and 7 of the fluorophore. Scheme 2 shows the synthesis of the prototype **5** and its acyl-bearing analog **4**.^[9]

The fluorescence properties of **5** were found to be rather different from those of compound **4**. As shown in Table 1, **5**



Scheme 2. Preparation of **4** and **5** (*p*-TSA = *p*-toluenesulfonic acid, TMEDA = *N,N,N',N'*-tetramethylethylenediamine).

Table 1. Spectroscopic properties of **4** and **5**.

Solvent		λ_{abs} [nm]	λ_{em} [nm]	τ_{F} [ns]	ϵ [M ⁻¹ cm ⁻¹]	Φ_{F}	$\epsilon \cdot \Phi_{\text{F}}$ [M ⁻¹ cm ⁻¹]
dichloromethane	4	449	561	24.4	4400	0.35	1540
	5	425	512	18.3	2300	0.77	1800
acetonitrile	4	444	561	20.3	4100	0.57	2300
	5	385	495	14.3	2800	0.55	1500
ethanol	4	452	596	11.6	4300	0.11	473
	5	384	510	13.3	3800	0.63	2400
methanol	4	452	611	5.9	4300	0.06	258
	5	384	509	13.3	4400	0.55	2500
H ₂ O	4 ^[a]	–	–	–	–	–	–
	5	370	488	20.2	4600	0.82	3800

[a] Insoluble in water.

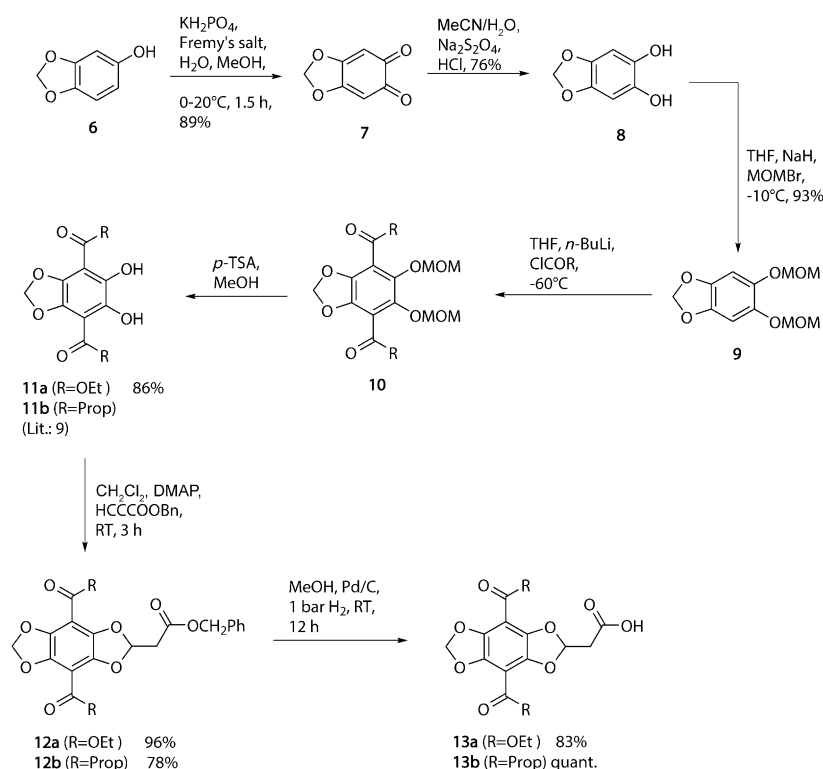
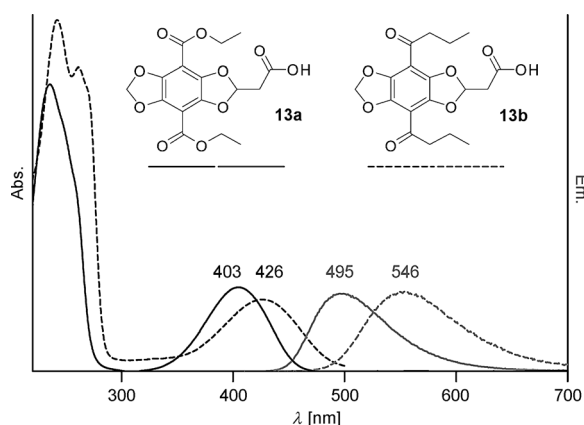
features a much higher fluorescence quantum yield and longer fluorescence decay in polar solvents than its acyl-bearing analog **4**.

Furthermore, it was observed that the fluorescence quantum yield and lifetime of compound **5** increases even further in water, whereas these values decrease drastically for water-soluble acyl-DBD derivatives (≈ 1.5 ns).^[11]

These results encouraged us to develop bioreactive derivatives that can be used as labels for proteins or other biological targets. Because of their own reactivity, carboxylic groups functioning as EWGs, these were found not to be ideal residues for more complex compounds containing bioreactive groups. Therefore, we replaced them with esters, expecting these compounds to show spectroscopic properties similar to those of **5**, but to be less reactive at their EWGs. We were able to synthesize compound **13a**, which bears ethyl esters as EWGs and a single reactive carboxylic function separated from its fluorophore (Scheme 3).

Starting from sesamol **6**, we optimized the synthetic route to the methoxymethyl (MOM)-protected catechol **9** used before for acyl-DBD dyes, and managed to introduce the desired ethyl esters (**10a**).^[13] After cleavage, catechol **11a** was cyclized with benzyl-protected propionic acid by using 4-dimethylaminopyridine (DMAP).^[9,14] Benzyl as a protecting group turned out to be superior to a methyl ester because the subsequent cleavage, leading to **13a** through hydrogenolysis, gives much higher yields than saponification. To compare both generations of DBD dyes, we also synthesized butyryl-DBD **13b** starting from the previously described catechol **11b**.^[9]

Figure 1 shows the typical absorption and emission spectra of DBD fluorophores. Similarly to acyl-DBD dyes (dotted), the $n-\pi^*$ absorption bands of ester-DBD dyes (solid) are broad and surprisingly intense. The latter bands are slightly hypso-

Scheme 3. Preparation of **13**.Figure 1. Absorption (black) and emission (gray) spectra of ester-DBD **13a** (solid) and acyl-DBD **13b** (dotted) in MeCN.

chromically shifted compared with those of acyl-DBD dyes, and give absorption maxima around 400 nm and emission maxima with equally broad bands around 500 nm.

The spectroscopic properties of compound **13a** and its equivalent acyl-DBD dye **13b** in various solvents (as shown in Table 2) substantiate the assumption that highly polar environments do not strongly reduce the fluorescence lifetime and intensity for this new generation of DBD dyes. In fact, water even increases the fluorescence lifetime by a few nanoseconds and preserves the high fluorescence quantum yield.

To shed light on the reasons for the different photophysical properties of acyl- and ester-DBD dyes, we performed DFT calculations with the model compounds **14** and **15**.

After geometry optimization (B3LYP/6-31G*), the 30 lowest-energy excited singlet states of **14** and **15** were calculated by using time-dependent (TD) DFT theory (TD-B3LYP/6-311++G**).^[15] The calculated wavelengths of the lowest-energy transition (**14**: 447.8 nm, **15**: 425.8 nm) are in fairly good agreement with the experimental UV data of **4**, **5**, and **13**. In particular, the considerably shorter absorption wavelength of ester-DBD compared with acyl-DBD is reproduced correctly. In both cases, the transition dipole moment is located in the π -plane of the molecules and follows a line connecting

Table 2. Spectroscopic properties of **13a** and **13b**.

Solvent		λ_{abs} [nm]	λ_{em} [nm]	τ_{F} [ns]	ϵ [M ⁻¹ cm ⁻¹]	Φ_{F}	$\epsilon \cdot \Phi_{\text{F}}$ [M ⁻¹ cm ⁻¹]
dichloromethane	13b	439	548	24.8	4300	0.35	1505
	13a	406	488	17.8	3105	0.75	2329
acetonitrile	13b	426	545	21.4	5683	0.41	2330
	13a	403	495	15.4	4680	0.56	2621
ethanol	13b	435	578	9.8	2183	0.18	393
	13a	408	508	17.6	5109	0.63	3219
methanol	13b	435	603	4.7	2110	0.08	169
	13a	407	508	16.9	5050	0.59	2980
H ₂ O	13b	446	640	1.5	–	< 0.05	–
	13a	414	528	20.5	4947	0.63	3117

the acetal C atoms (Figure 2).

A remarkable difference between acyl- and ester-DBD chromophores can be derived from the details of the lowest-energy transitions. In the case of **14**, this transition is affected solely by an excitation from the HOMO (No. 65) to the LUMO (No. 66). This excitation is accompanied by a shift of the electron density from the [1,3]dioxolo[4,5-*f*]-[1,3]benzodioxole moiety to the acyl groups, which is clearly discernible by visualizing these orbitals (Figure 3).

In contrast to **14**, the lowest-energy transition of ester-DBD **15** is actually a mixture of the same HOMO–LUMO excitation (73→74, CI coefficient 0.7233) and an excitation from HOMO–1 to LUMO+4 (72→78, CI coefficient –0.10402). The latter excitation is characterized by a shift of the electron density in the opposite direction, that is, from

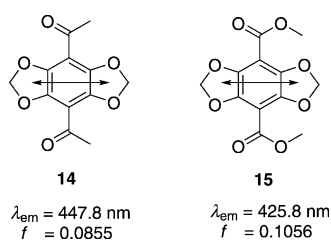


Figure 2. Transition dipole moment (arrows), calculated absorption wavelength and oscillator strength of the lowest-energy transition of **14** and **15**.

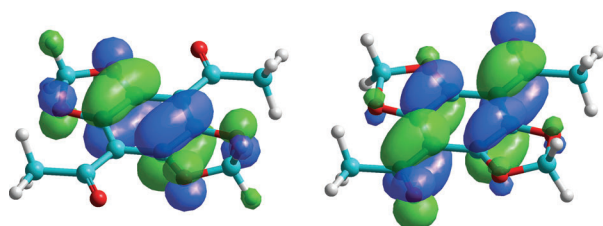


Figure 3. HOMO (left) and LUMO (right) of acyl-DBD dye **14**.

the ester groups to the [1,3]dioxolo[4,5-*f*][1,3]benzodioxole moiety (Figure 4).

We hypothesize that the different nature of the lowest-energy transitions of acyl- and ester-DBD dyes is responsible for the differences between their photophysical properties.

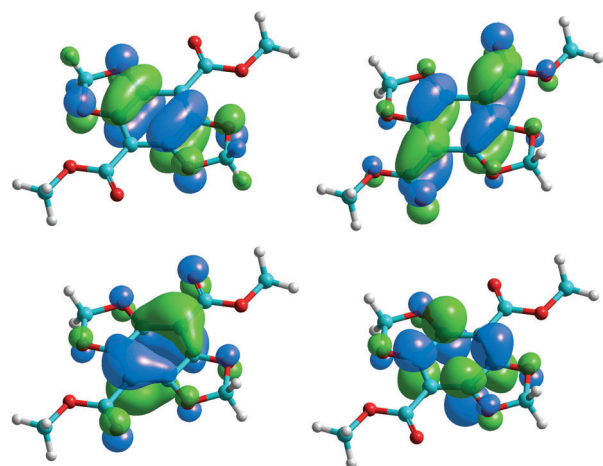


Figure 4. HOMO (top left), LUMO (top right), HOMO-1 (bottom left), and LUMO+4 (bottom right) of ester-DBD dye **15**.

Photostability: Another important parameter for fluorescent dyes is their photostability. Owing to the unusual combination of large Stokes shifts, long fluorescence lifetimes, and high fluorescence quantum yields, it is difficult to compare DBD dyes with other commonly used fluorophores. However, we try to give a reference point in terms of the behavior of DBD dyes concerning the issue of photostability. Therefore, we chose to compare them with two derivatives of

widely used fluorophores that show at least similar absorption and emission maxima, that is, 4-*N*-propargyl NBD **16a** and 5-propargylamido-carboxyfluorescein **16b**, respectively. Figure 5 illustrates the photobleaching of DBD dyes **13a** and **13b** observed through the decrease in their absorption maxima (403, 426 nm) compared with **16a** and **16b** at one of their significant absorption maxima (330, 500 nm), upon exposure to a 500 W mercury arc lamp combined with a 290 nm edge filter (see the Supporting Information for experimental details). It is seen that acyl DBD **13b** shows a higher photostability than NBD dye **16a** and a similar behavior to the carboxyfluorescein derivative **16b**. Ester DBD **13a** is even less photolabile under the experimental conditions used.

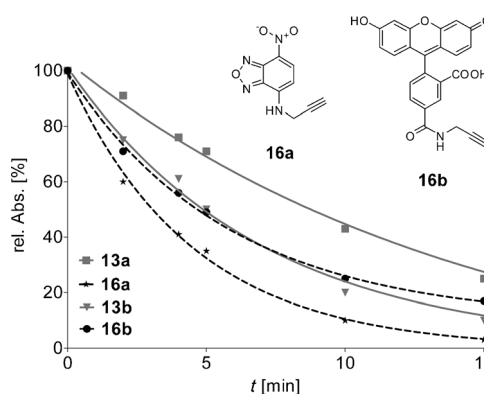
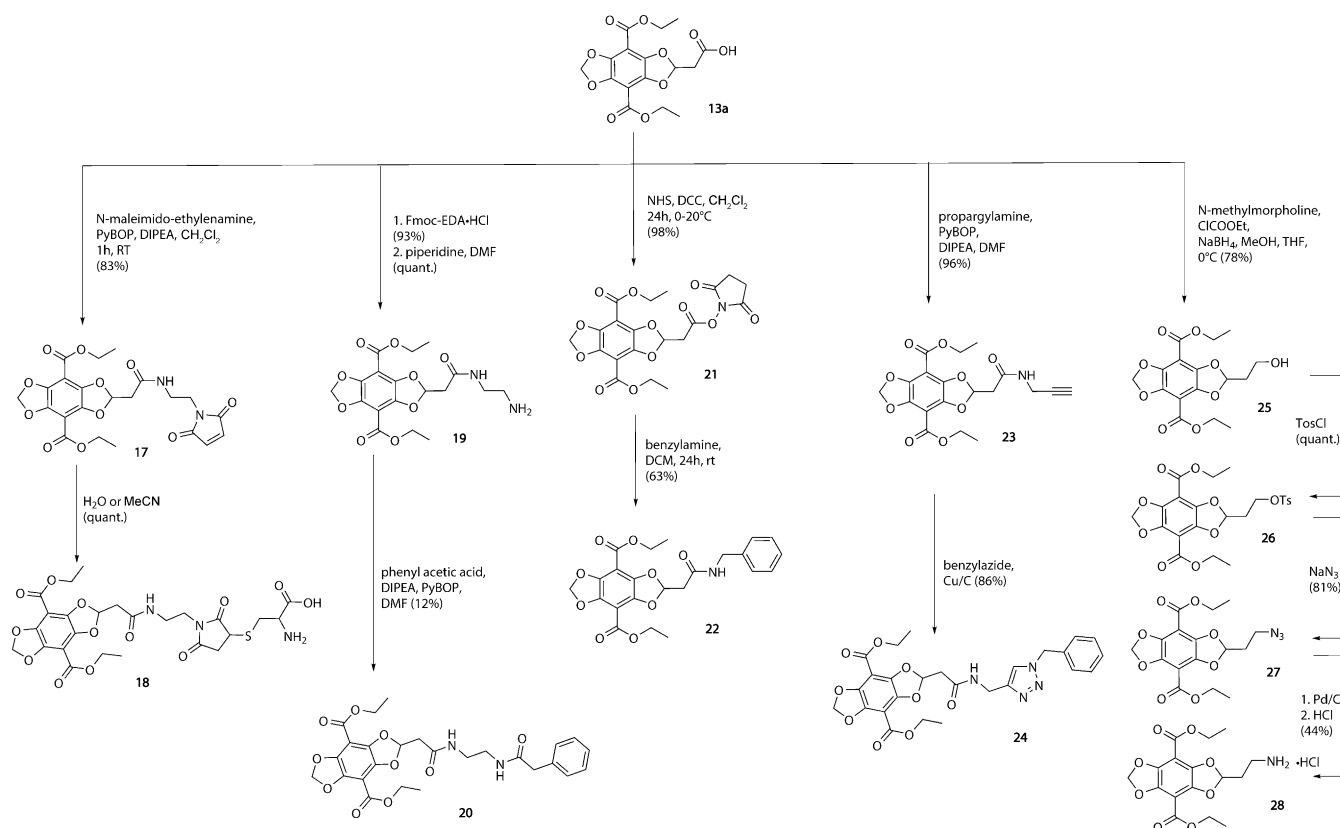


Figure 5. Photobleaching of **13a** (■), **13b** (▼), **16a** (★), and **16b** (●) in acetonitrile (dye concentration: $1 \times 10^{-4} \text{ M}$).

Biofunctionalized ester-DBD dyes: We then decided to take advantage of these positive parameters of DBD esters. As mentioned above, the combination of photostability and high fluorescence quantum yields in addition to long fluorescence lifetimes and large Stokes shifts is rare, and should be interesting for new probes for bioanalytical issues. Thus, various functional derivatives of **13a** bearing bioreactive residues were synthesized successfully (Scheme 4). Because of their small molecular size, these derivatives should be able to approach small protein pockets and other less accessible domains.^[16] Scheme 4 shows the synthetic routes to ester-DBD dyes bearing maleimido (**17**), NHS ester (**21**), alcohol (**25**), azide (**27**), alkyne (**23**), sulfonate ester (**26**), and amino groups (**19**, **28**). The synthesis of most bioreactive compounds is based mainly on classic peptide-coupling techniques.^[17] Through optimization of the reaction conditions and the testing of different coupling agents, it was possible to obtain all the compounds in good to excellent yields. Alcohol **25** was accessible by using a NaBH_4 -provided reduction under mild conditions, as described by Kokotos et al.^[18]

These functionalized derivatives could react with corresponding groups such as thiols, amines, carboxylic acids, alkynes, and azides, which are often targets in biological structures.^[19] This was proven through sample reactions with simple compounds containing such target groups.



Scheme 4. Bioreactive derivatives of **13a** (PyBOP = (benzotriazol-1-yloxy)tripyrrolidinophosphonium hexafluorophosphate, DIPEA = diisopropylethylamine, Fmoc-EDA = *N*-(9-fluorenylmethyloxycarbonyl)ethylenediamine, NHS = *N*-hydroxysuccinimide, DCC = dicyclohexylcarbodiimide, Tos = 4-toluene-sulfonyl).

Fluorescence quenching of DBD dyes caused by maleimides: Along with the other biofunctionalized compounds, maleimide **17** drew particular attention because its C=C double bond can undergo selective addition reactions with thiols.^[20]

Because accessible thiol groups in proteins are relatively rare and of great interest, it was promising to attempt the use of DBD-maleimides as probes working in thiol-containing domains of proteins.^[21–24]

Thiols, also known as sulfhydryls, often exist in proteins under reducing conditions, but are more often found in native proteins in their oxidized form as disulfide bridges. The latter play an important role in the tertiary structure of, for example, antibodies. Labeling of these protein domains requires cleavage of the disulfide bonds by reducing agents to obtain the free thiol groups.^[25] This technique is commonly followed by labeling of the hinge region of antibodies. Another field of interest is the labeling of artificially introduced cysteine residues inside peptide chains.^[26–28] Here, the aim is to place a reactive thiol close to a domain where a maleimide-functionalized probe could gather information about its surroundings. Therefore, we intended to investigate whether DBD dyes have the potential to fulfill such a task. To obtain **17**, we needed to synthesize a maleimide derivative bearing a short linker with a nucleophilic amine at its end. This linker is important because the often buried thiol groups in proteins are more accessible if the maleimide is

not attached directly to the probe.^[29] Starting from *tert*-butylcarbamate (Boc)-protected ethanol-amine, we substituted the hydroxyl group by a maleimido residue by using a Mitsunobu reaction.^[30] After deprotection, the resulting 2-maleimido-ethylenamine was reacted with **13a** by using a peptide-coupling strategy involving (benzotriazol-1-yloxy)tripyrrolidinophosphonium hexafluorophosphate (PyBOP) as a coupling agent.

We first investigated the spectroscopic properties of **17** in detail. It is known that maleimides often quench the luminescence of chromophores,^[23,31,32] and as compound **17** shows almost no fluorescence at all, it is indicated that such quenching is observed here. The fluorescence intensity and lifetime of **17** increase strongly upon reaction of the double bond of the maleimide with a thiol (e.g., cysteine) to form the corresponding thioether **18**. Because of the interruption of the former conjugated π -system, quenching is now prevented (Figure 6).

It is important to stress that the detected fluorescence of maleimide **17** is actually the signal of the already reacted maleimide with some impurities. We assume that intramolecular quenching of pure **17** is so efficient as to be close to one hundred percent. Otherwise, the detected fluorescence decay of **17** seen in Figure 6 would not show such a sharp edge but monoexponential behavior. As described by Guy et al. and Maeda et al., the quenching by maleimides does not involve singlet deactivation through intersystem crossing

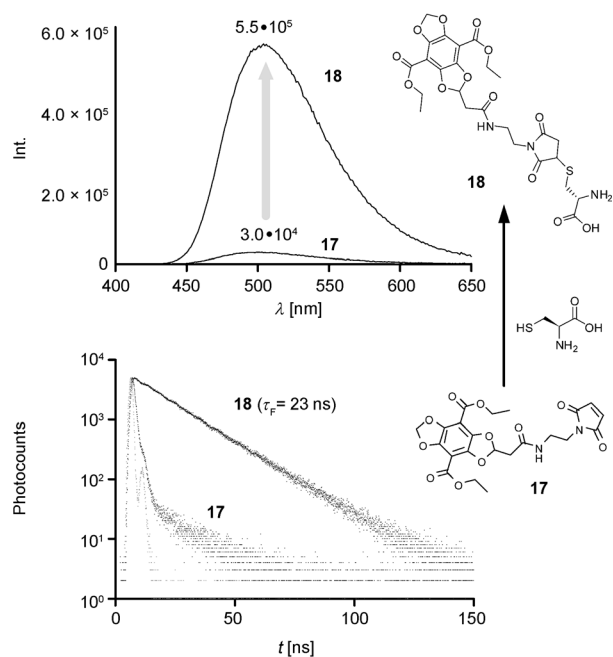


Figure 6. Fluorescence intensity and lifetime of maleimide **17** and its corresponding Cys-thioether **18** in water/acetone (1:1).

(ISC).^[23,33] Because of the lack of matching absorption and emission spectra, Förster resonance energy transfer (FRET) between **13a** and a maleimide can also be ruled out.^[34,35a] Instead, deactivation through photoelectron transfer (PET) is assumed.

For a consideration of whether the fluorophore and a maleimide (we chose *N*-methylmaleimide, NMM) are compatible for PET, their electron donor and acceptor levels must be compared by using the Rehm–Weller equation [Eq. (1)].

$$\Delta G = E(D^+/D) - E(A/A^-) - \Delta G_{00} - (e^2/\epsilon d) \quad (1)$$

Here, $E(D^+/D)$ is the oxidation potential of the fluorophore, $E(A/A^-)$ the reduction potential of the quencher, ΔG_{00} the energy difference between the ground and excited state, and $(e^2/\epsilon d)$ the reorganization energy. The latter coulomb term can be simplified to a value of 1.3 kcal mol⁻¹ for acetonitrile, because it has a minor influence compared with other thermodynamic parameters.^[35b] ΔG_{00} can be derived from the point of intersection between the normalized absorption and emission spectra of the fluorophore. For **13a**, this value was found to be 460 nm (62.2 kcal mol⁻¹). The redox potentials of **13a** were determined through cyclic voltammetry (Figure 7, vs. NHE), which gave an oxidation potential of 1.03 V (23.8 kcal). The reduction potential of NMM was determined to be -1.185 V (-27.21 kcal). It was calculated that an electron transfer from **13a** to NMM is energetically preferred ($\Delta G = -12.51$ kcal mol⁻¹).

To confirm these results further, we investigated whether the steady-state fluorescence and fluorescence lifetime decrease when the quencher (NMM) is added to a solution of **13a** in MeCN. This Stern–Volmer experiment was expected

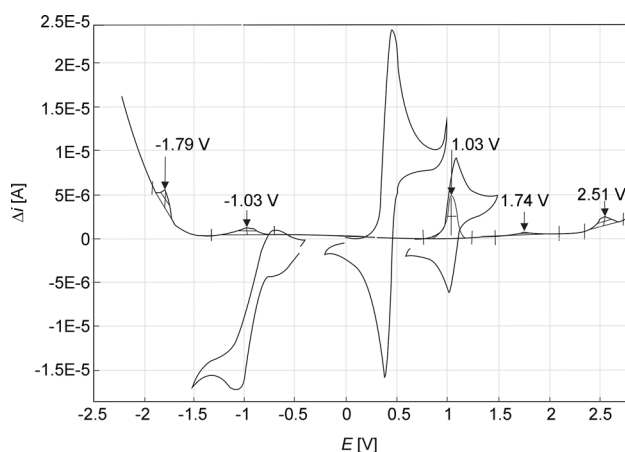


Figure 7. Cyclic voltammogram of **13a** in MeCN: reversible oxidation stage at 1.03 V; quasi-reversible reduction stage at -1.03 V.

to give information about the quenching kinetics, and should confirm the assumed PET mechanism.^[36] As Figure 8 illustrates, the fluorescence intensity of **13a** is reduced with increasing concentrations of NMM. We then determined the Stern–Volmer quenching rate K_{SV} by plotting the decreasing fluorescence lifetime against the NMM concentration (inset of Figure 8).

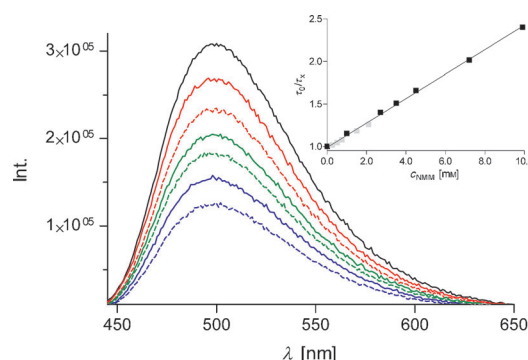


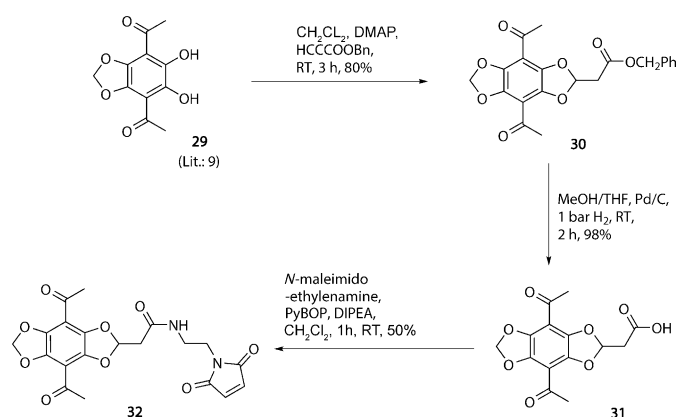
Figure 8. Titration of **13a** with various amounts of *N*-methyl-maleimide (NMM) in MeCN: 0.0 mM (black), 1.0 mM (red), 2.7 mM (red, dotted), 3.5 mM (green), 4.5 mM (green, dotted), 7.2 mM (blue), 9.9 mM (blue, dotted).

The derived slope is K_{SV} (144 M⁻¹), which, divided by the monoexponential fluorescence lifetime of **13a** (15.4 ns), gives the second-order quenching rate k_q . The determined value for **13a** (9.35×10^9 M⁻¹ s⁻¹) is near the diffusion limit of the solvent, which is consistent with a fast quenching mechanism such as PET. The fact that the emission maxima did not shift at any given NMM concentration but that the fluorescence lifetime decreased strongly indicates that the quenching must be a dynamic process.^[37]

Besides the ester-DBD **13a**, identical measurements and calculations were made for the equivalent acyl-DBD **13b**, and similar results were obtained (see the Supporting Information for details).

Hence, we were able to confirm PET as the preferred quenching mechanism for ester- and acyl-DBD fluorophores in the presence of maleimides.

Maleimido-DBD dyes as fluorescence lifetime probes for monitoring conformational changes in proteins: This very effective fluorescence quenching of DBD-maleimides allowed these probes to report clearly when any bonding to corresponding thiols actually occurred, because only then is the fluorescence detectable.^[21] We expected that maleimides of both generations would show distinct fluorescence lifetime changes upon a change in their microenvironment creating a new surrounding polarity. To probe this, we chose the well-characterized maltose ATP-binding cassette transporter MalFGK₂ as a biological test system, taking **17** and **32** (Scheme 5) as promising representative labels. MalFGK₂



Scheme 5. Synthesis of maleimide **32**.

is a worthwhile target protein, because studies on the conformational change during the transition from the cofactorless state (apo-state) to an intermediate ATP/ADP-bound state (trap-state), which is acquired by adding vanadate to the ATP hydrolyzing transport complex (see the Supporting Information), have been performed previously by limiting proteolysis and using steady-state fluorescence spectroscopy.^[28] The transport complex to which the substrate is delivered by maltose binding protein (MBP) consists of one copy of each of the transmembrane subunits (MalF and MalG) and two copies of the nucleotide-binding subunit (MalK).

The binding of the nucleotide to MalK causes a conformational change in two tryptic cleavage sites in the periplasmic loops (P2 of MalF and P1 of MalG). The previously constructed variant Ser²⁵²Cys of MalF located ten residues apart from the putative tryptic cleavage site; Lys²⁶² was used for labeling this subdomain with DBD-maleimides.^[28] Exemplarily for both probes, Figure 9 illustrates schematically the location of **17** in the maltose ABC transporter.

Figure 10 presents the fluorescence lifetime signals detected from both probes as well as the shifts of the emission maxima. The average fluorescence lifetime of **32** increases by more than 1 ns up to 6.3 ns when MalF is in the trap-

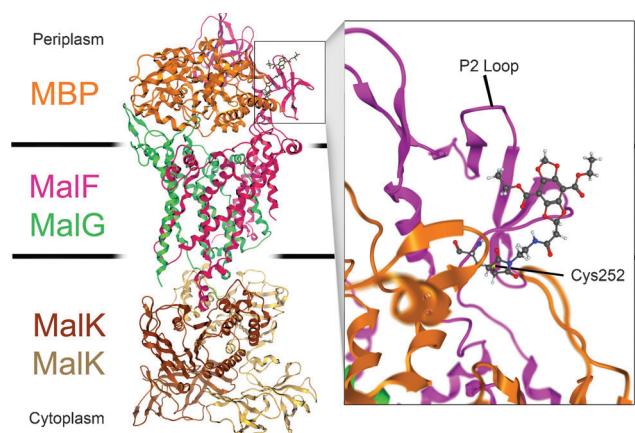


Figure 9. Simulation of the location of **17** in MalF(S252C)GK₂ (pdb 3PV0). The transporter is trapped in an intermediate prehydrolytic form.^[38]

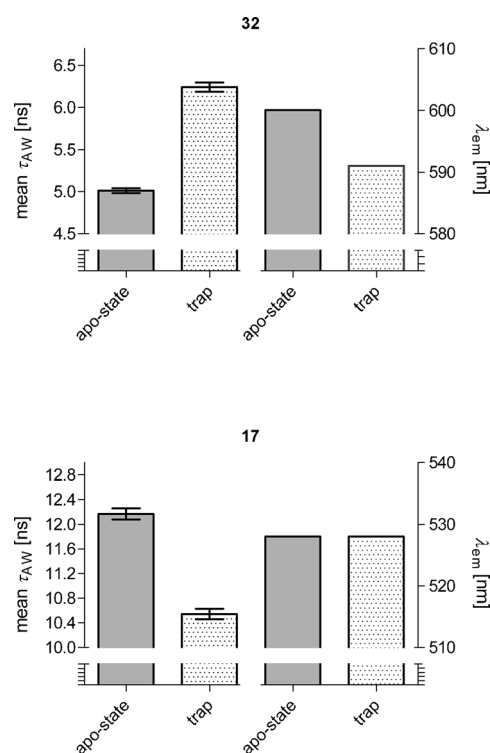


Figure 10. Changes in fluorescence lifetimes and emission maxima of **32** and **17** located in MalF(S252C)GK₂ (apo and trap forms).

state conformation. In line with previous data, this conformation presumably creates a more apolar microenvironment to which the probe responds.^[28] As expected, the opposite signal-change tendency is observed for **17**. Here, the fluorescence lifetime is reduced by 1.6 ns in the trap-state of MalF. However, the value is still very high (10.4 ns) and far from any background fluorescence decay. The according behavior of both probes is also observed in the shift of the emission maxima, as expected from the spectroscopic measurements of the original compounds (Table 2). Whereas **32** shows a significant blueshift of 9 nm in the trap-state, which again con-

firming its movement to a more apolar environment, **17** does not display such behavior, as the spectrum is insensitive to changes in polarity. These findings correlate perfectly with previous observations proving that the orthogonal behaviors of acyl- and ester-DBDs concerning fluorescence lifetime changes make them a very handy tool, as they deliver a sensitive positive/negative control.

These results encouraged us to adapt the approach to another system that performs larger and well-studied movements: the maltose-binding protein MBP. Figure 11 illus-

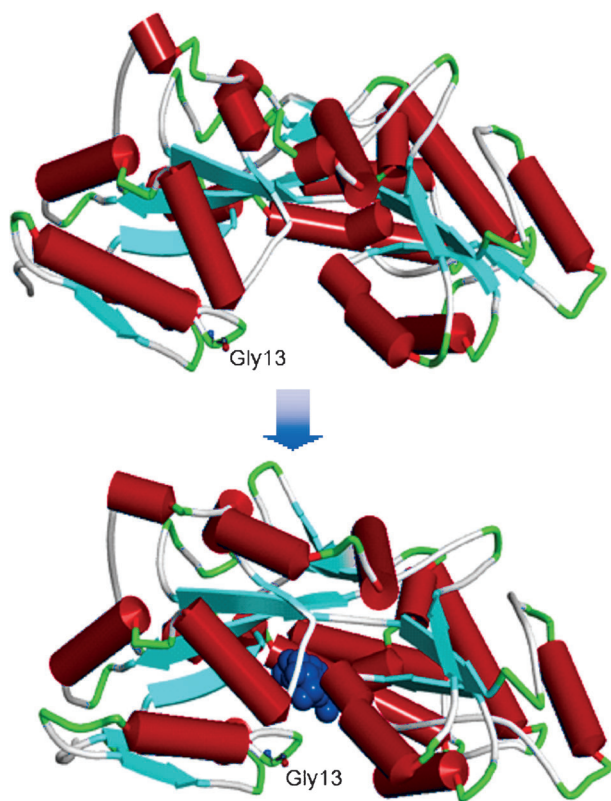


Figure 11. The N- and C-lobes of maltose-binding protein reside in an “open” conformation in the absence of a ligand (top) and change conformation to a “closed” form upon trapping of maltose (blue, “Venus fly-trap” model; bottom). The location of Gly13 residues is indicated and maltose is shown in space-filling representation (in blue). Pdb files 1N3X (open) and 1ANF (closed).^[39,40]

trates the conformational change of MBP resulting from the binding of maltose and the location of Gly¹³ at the entrance of the maltose-binding pocket. Gly¹³ changes its relative position significantly during the transition from the open to the closed conformation. Substitution of this glycine with cysteine (Gly¹³Cys) provides a protein that can be labeled with **17** and **32**, respectively, monitoring the changes in the specific microenvironment. The labeled variant retained its ability to bind maltose, as verified through its binding to an amylose matrix and elution with maltose (see the Supporting Information).

The **17**- and **32**-labelled Gly¹³Cys variant displays fluorescence lifetime changes (Figure 12) that suggest that the envi-

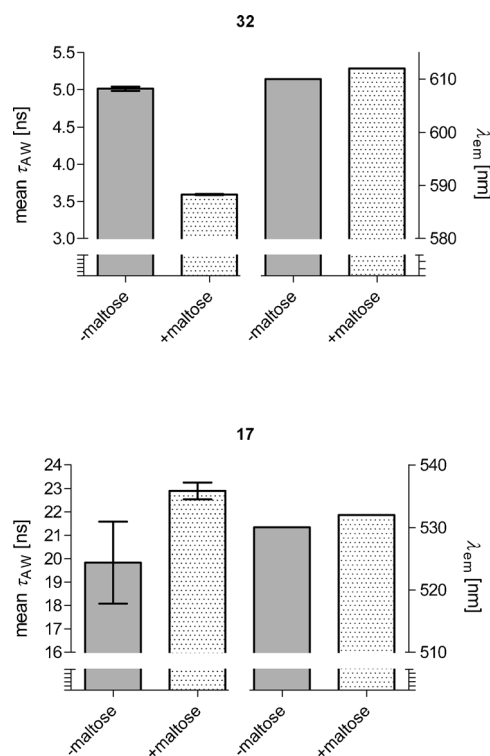


Figure 12. Changes in fluorescence lifetimes and emission maxima of **32** and **17** located in MalE(G¹³C) (maltose ligated and unligated form).

ronment changes from apolar to polar as the lobes of MBP close, because the fluorescence lifetime of **32** decreases by 1.3 ns and that of **17** increases by about 3 ns after the addition of maltose. The reciprocal behavior of the two maleimide labels provides internal confirmation of the consistency of these data, which is consistent with the shift of the emission maxima to longer wavelengths by 4 nm with **32** in the closed conformation, whereas those of **17** remain constant. However, the opposite result could have been proposed with a more packed yet more apolar neighborhood of this position in the ligand form of MBP.

Apparently, the Gly¹³Cys position bends towards a more polar ambit. The fluorophore is probably oriented outward, toward the interface between MBP and the transmembrane subunits, thus preventing productive interaction. Together, both test systems confirm the suitability of the developed maleimido-DBD dyes for monitoring microenvironmental changes in biological samples, providing an internal control through their juxtaposing behavior and giving precise and reliable information thanks to their long but sensitive fluorescence lifetimes.

Conclusion

We have presented the synthesis and spectroscopic properties of novel fluorophores containing a [1,3]dioxolo[4,5-*f*]-[1,3]benzodioxole (DBD) backbone. In comparison with

previously described DBD dyes, they show long fluorescence decay and high quantum yields, even in aqueous solutions. Furthermore, they can be functionalized for reaction with biomolecular targets. Maleimido derivatives of both generations were shown to undergo a photoelectron transfer (PET) quenching manifold. We labeled these dyes to protein pockets containing a central thiol group and investigated their spectroscopic behaviors during conformational changes in the proteins. In combination, ester- and acyl-DBD dyes are a sensitive toolkit for monitoring microenvironmental changes in biological samples, providing an internal control due to the juxtaposition of their fluorescence lifetime behaviors.

Acknowledgements

We thank Dr. W. Mickler for performing the cyclovoltammometric measurements and Katlen Brennenstuhl for performing the fluorescence quantum yield measurements.

- [1] M. Y. Berezin, S. Achilefu, *Chem. Rev.* **2010**, *110*, 2641–2684.
- [2] J. W. Borst, A. Visser, *Meas. Sci. Technol.* **2010**, *21*, 102002.
- [3] R. N. Dsouza, U. Pischel, W. M. Nau, *Chem. Rev.* **2011**, *111*, 7941–7980.
- [4] S. C. Mondal, K. Sahu, K. Bhattacharyya, in *Reviews in Fluorescence 2007* (Ed.: C. D. Geddes), Springer, New York, **2009**, pp. 157–177.
- [5] G. Bains, A. B. Patel, V. Narayanaswami, *Molecules* **2011**, *16*, 7909–7935.
- [6] M. Beija, C. A. M. Alfonso, J. M. G. Martinho, *Chem. Soc. Rev.* **2009**, *38*, 2410–2433.
- [7] B. D. Wagner, *Molecules* **2009**, *14*, 210–237.
- [8] C. Sun, J. Yang, L. Li, S. Lui, *J. Chromatogr. B* **2004**, *803*, 173–190.
- [9] P. Wessig, R. Wawrzinek, K. Möllnitz, E. Feldbusch, U. Schilde, *Tetrahedron Lett.* **2011**, *52*, 6192–6195.
- [10] P. Wessig, R. Wawrzinek, K. Möllnitz, EP2399913 A1, **2010**.
- [11] R. Wawrzinek, P. Wessig, K. Möllnitz, J. Nikolaus, R. Schwarzer, P. Müller, A. Herrmann, *Bioorg. Med. Chem. Lett.* **2012**, *22*, 5367–5371.
- [12] E. Bordignon, M. Grote, E. Schneider, *Mol. Microbiol.* **2010**, *77*, 1354–1366.
- [13] Y. Q. Ye, H. Koshino, J. Onose, K. Yoshikawa, N. Abe, S. Takahashi, *Org. Lett.* **2007**, *9*, 4131–4134.
- [14] M.-J. Fan, G.-Q. Li, L.-H. Li, S.-D. Yang, Y.-M. Liang, *Synthesis* **2006**, *14*, 2286–2292.
- [15] M. A. L. Marques, C. A. Ullrich, F. Nogueira, A. Rubio, K. Burke, E. K. U. Gross, *Time-Dependent Density Functional Theory*, Springer, Heidelberg, **2006**.
- [16] T. Kawabata, N. Go, *Proteins Struct. Funct. Bioinf.* **2007**, *68*, 516.
- [17] A. El-Faham, F. Albericio, *Chem. Rev.* **2011**, *111*, 6557–6602.
- [18] G. Kokotos, *Synthesis* **1990**, *4*, 299–301.
- [19] G. T. Hermanson, *Bioconjugate Techniques*, 2nd ed., Elsevier, Amsterdam **2008**, p. 169.
- [20] C. F. Brewer, J. P. Riehm, *Anal. Biochem.* **1967**, *18*, 248–255.
- [21] K. Huang, W. Bulika, A. Marti, *Chem. Commun.* **2012**, *48*, 11760–11762.
- [22] X. Wang, S. Wang, H. Ma, *Analyst* **2008**, *133*, 478–484.
- [23] J. Guy, K. Caron, S. Dufresne, S. W. Michnick, W. G. Skene, J. W. J. Keillor, *J. Am. Chem. Soc.* **2007**, *129*, 11969–11977.
- [24] K. Tyagarajan, E. Pretzler, J. E. Wiktorowicz, *Electrophoresis* **2003**, *24*, 2348–2358.
- [25] R. Singh, G. V. Lamoureux, W. J. Lees, G. M. Whitesides, *Methods Enzymol.* **1995**, *251*, 167–173.
- [26] T. Kurpiers, H. Mootz, *Angew. Chem.* **2007**, *119*, 5327–5330; *Angew. Chem. Int. Ed.* **2007**, *46*, 5234–5237.
- [27] T. Kurpiers, H. Mootz, *ChemBioChem* **2008**, *9*, 2317–2325.
- [28] M. L. Daus, H. Landmesser, A. Schlosser, P. Müller, A. Herrmann, E. Schneider, *J. Biol. Chem.* **2006**, *281*, 3856–3865.
- [29] M. Link, X. Li, J. Kleim, O. S. Wolfbeis, *Eur. J. Org. Chem.* **2010**, 6922–6927.
- [30] C. Antczak, B. Bauvois, C. Monneret, J.-C. Florent, *Bioorg. Med. Chem.* **2001**, *9*, 2843–2848.
- [31] X. Chen, Y. Zhou, X. Peng, J. Yoon, *Chem. Soc. Rev.* **2010**, *39*, 2120–2135.
- [32] K. Caron, V. Lachapelle, J. W. Keillor, *Org. Biomol. Chem.* **2011**, *9*, 185–197.
- [33] H. Maeda, T. Maeda, K. Mizuno, K. Fujimoto, H. Shimizu, M. Inouye, *Chem. Eur. J.* **2006**, *12*, 824–831.
- [34] C. W. Miller, E. S. Jönsson, C. E. Hoyle, K. Viswanathan, E. J. Valente, *J. Phys. Chem. B* **2001**, *105*, 2707–2717.
- [35] J. R. Lakowicz, *Principles of Fluorescence Spectroscopy*, Springer, New York, **2006**; a) p. 443, b) p. 337.
- [36] O. Stern, M. Z. Volmer, *Phys. Z.* **1919**, *20*, 183–188.
- [37] L. K. Fraiji, D. M. Hayes, T. C. Werner, *J. Chem. Educ.* **1992**, *69*, 424–428.
- [38] M. L. Oldham, J. Chen, *Science* **2011**, *332*, 1202–1205.
- [39] P. G. Telmer, B. H. Shilton, *J. Biol. Chem.* **2003**, *278*, 34555–34567.
- [40] F. A. Quiocho, J. C. Spurlino, L. E. Rodseth, *Structure* **1997**, *5*, 997–1015.

Received: June 20, 2013
Revised: September 6, 2013
Published online: November 8, 2013